Electronic Supplementary Material (ESI) for Journal of Materials Chemistry B.

Supporting information

for

Shape-transformation of polymersomes from glassy ABA triblock copolymers

Tamuka Chidanguro, Elina Ghimire, and Yoan C. Simon*

School of Polymer Science and Engineering, The University of Southern Mississippi,

118 College Dr. #5050 Hattiesburg 39406 MS USA

*Author to whom correspondence should be addressed:

E-mail:yoan.simon@usm.edu

Table of contents

Synthesis and characterization of CMA

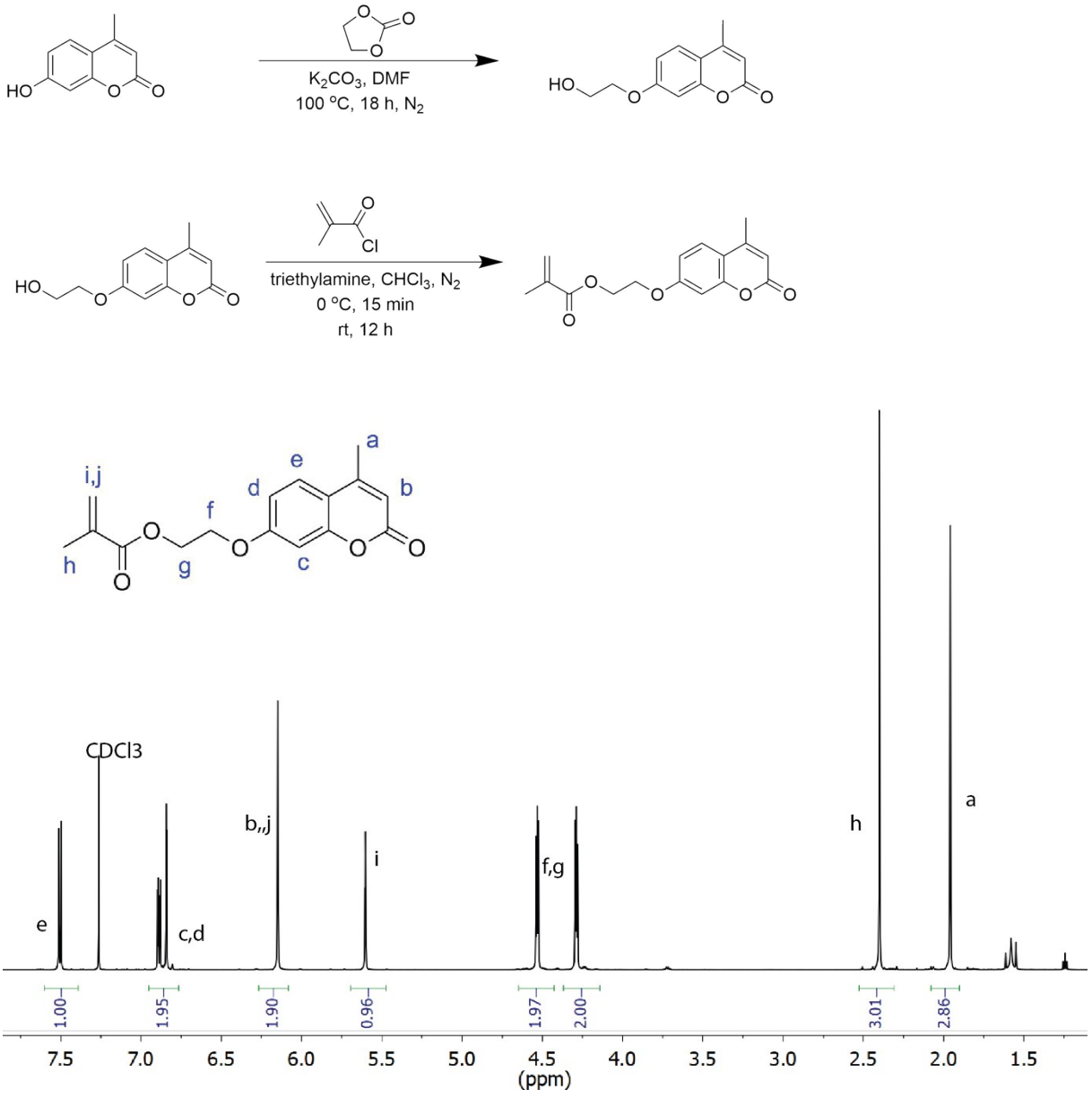

Figure S1. (Top) Synthesis of the coumarin methacrylate (CMA) monomer from the precursor (7-(2-hydroxyethoxy)-4-methylcoumarin. (Bottom) ^{1}H NMR spectrum of the monomer CMA.

Synthesis and characterization of diCEP

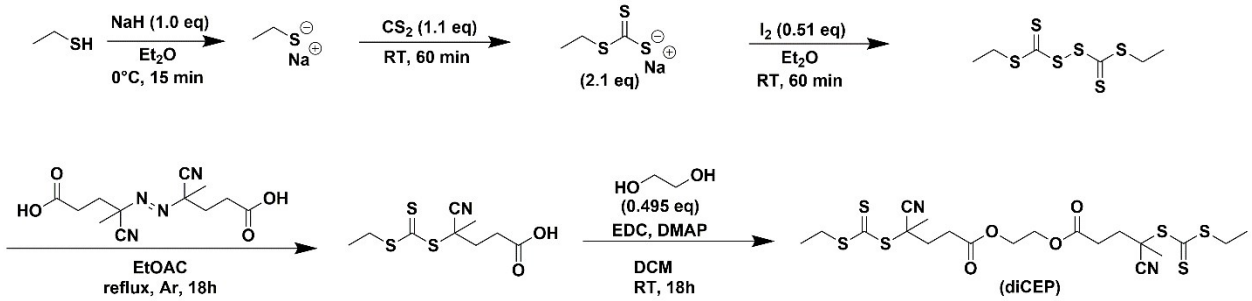

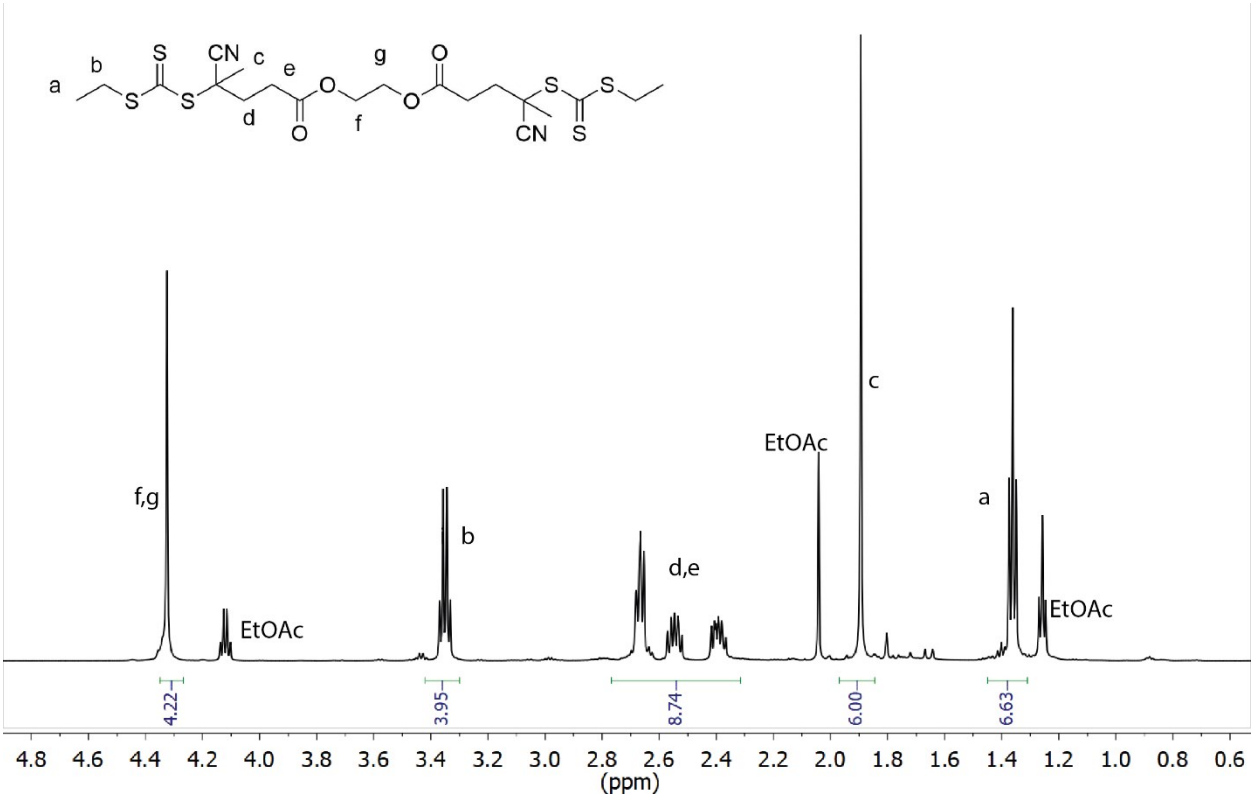

Figure S2. (Top) Synthesis of the difunctional CTA diCEP. (Bottom) ^{1}H NMR spectrum of diCEP.

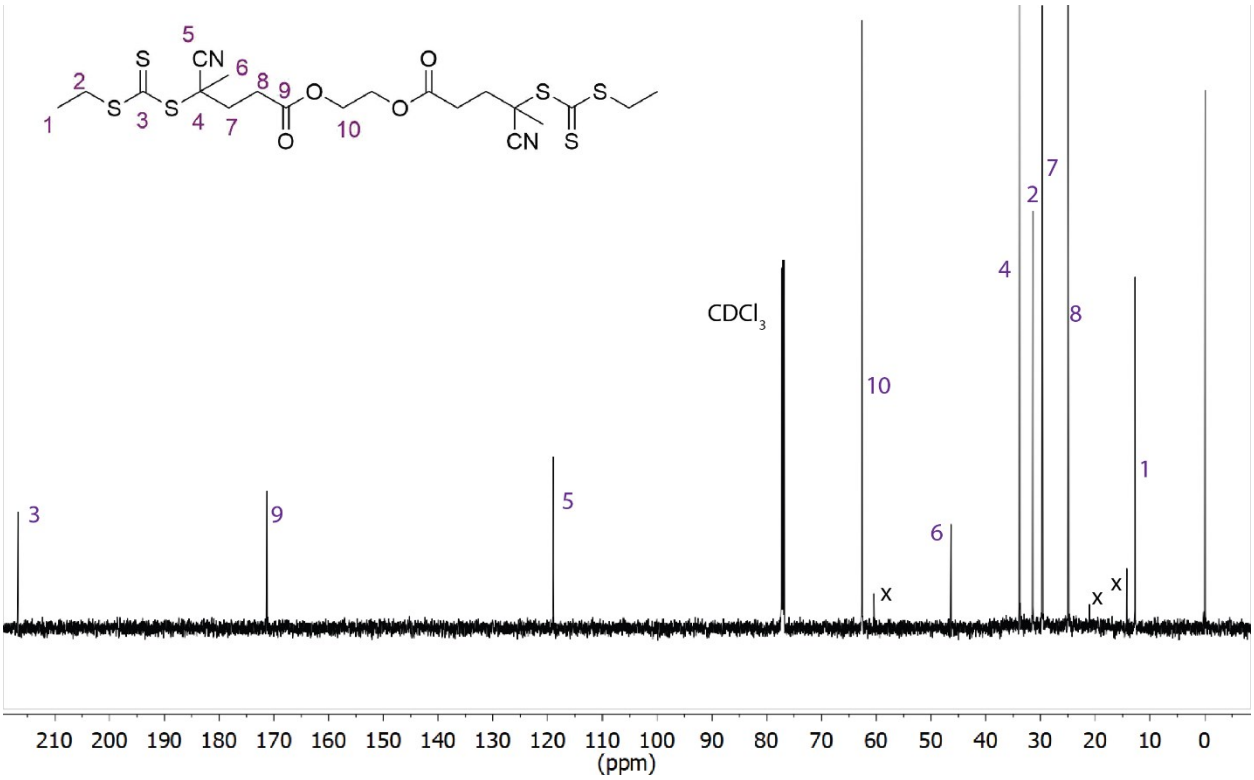

Figure S3. ^{13}C NMR spectrum of diCEP taken in $CDCl_3$. x represents residual ethyl acetate.

RAFT copolymerization of styrene and CMA and characterization of P(S-*stat*-CMA)

Calculation of the amount of CMA incorporated during RAFT copolymerization

The CMA incorporation was calculated based on the integration of the aromatic peaks (a, and h, in magenta in Scheme S3 below) and the alkene peak (j, in blue). For each repeat unit *(m + n =1)*:

the number of aromatic peaks = $3 \times n\ (from\ h) + 5 \times m\ (from\ a)$

$= 3n + 5(1 - n) = 5 - 2n$

the number of alkene protons = $1 \times n\ (from\ j) = n$

∴ for an aromatic ratio/alkene ratio, *y*, the CMA incorporated, $n = \dfrac{5}{(y + 2)}$ [S1]

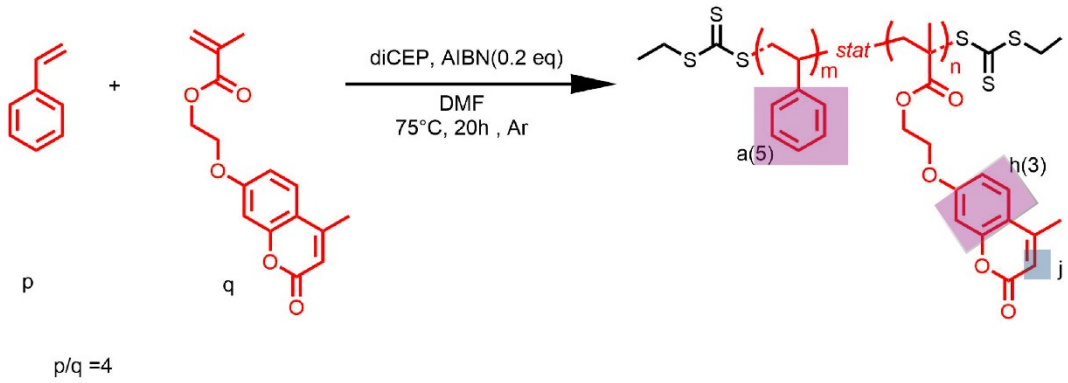

Scheme S1. Reaction scheme showing the RAFT copolymerization of styrene and CMA. The ratio of the aromatic regions (in magenta) to the alkene peaks (in blue) was used in the calculation of the amount of CMA incorporated into the polymer during the RAFT copolymerization.

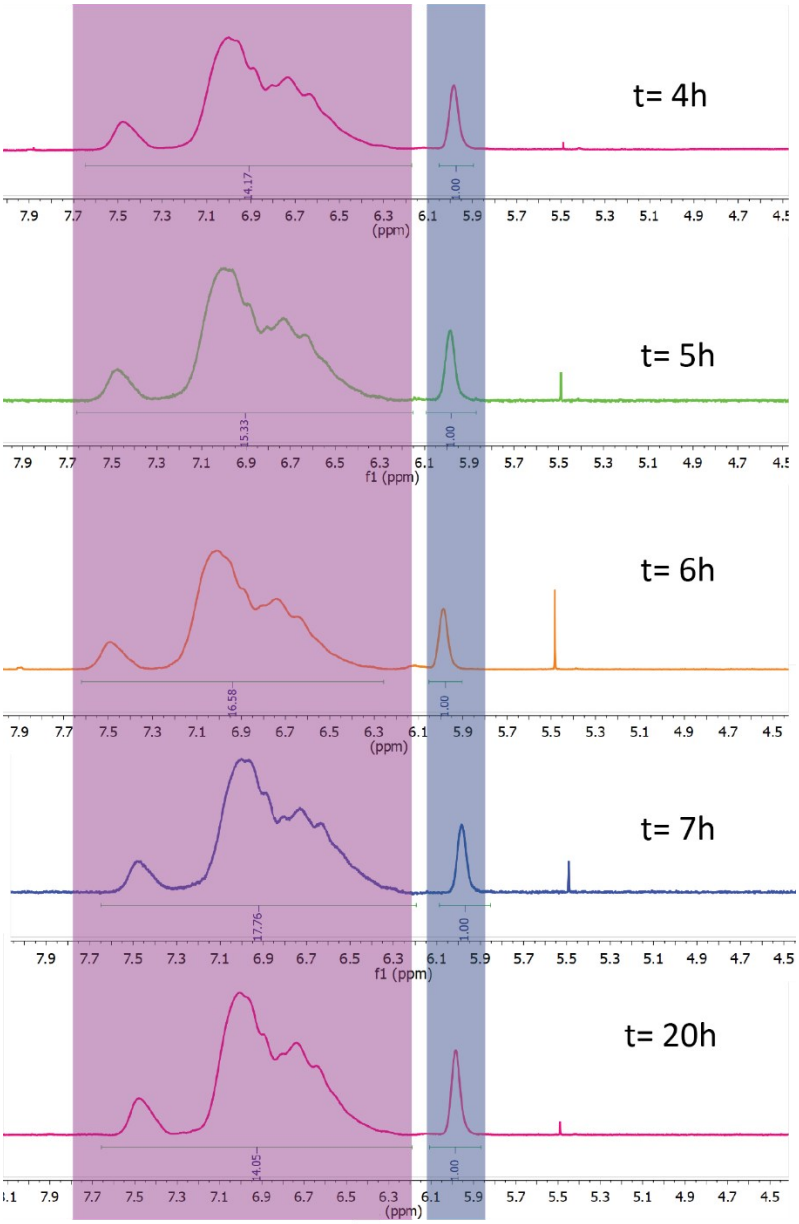

Figure S4. ^{1}H NMR spectra showing the copolymerization of styrene and CMA over time. The incorporation of CMA was calculated in Table S1 is based on the ratio of the alkene peak (in blue) to the aromatic region (in magenta).

Table S1. CMA incorporated into hydrophobic blocks as a function of time during the RAFT copolymerization of S and CMA.

Time point (h)	Aromatic/alkene ratio	CMA:styrene	Total CMA composition
4	14.17	1:2.23	0.31
5	15.33	1:2.45	0.29
6	16.58	1:2.72	0.27
7	17.76	1:2.95	0.25
20	14.05	1:2.21	0.31

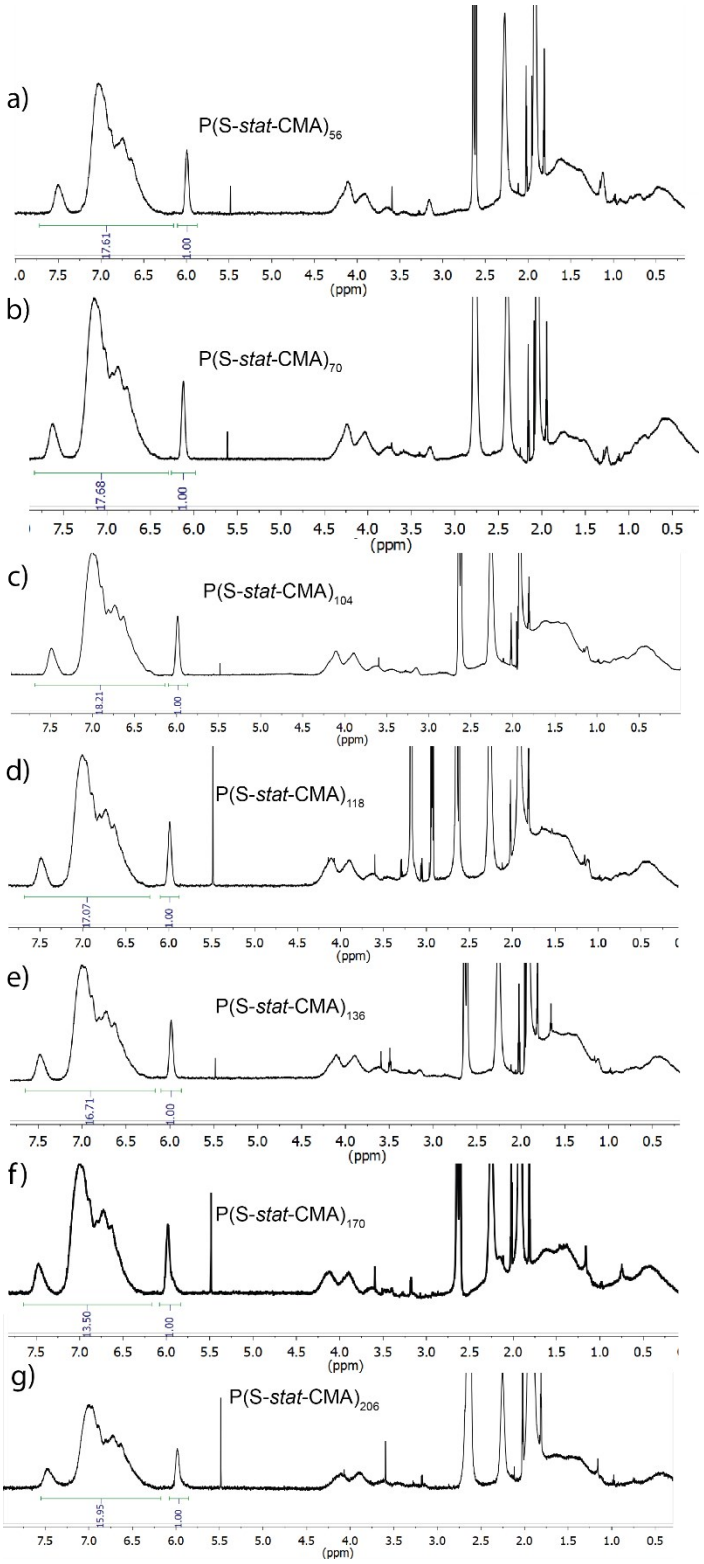

Figure S5. ^{1}H NMR spectra showing the aromatic/alkene ratio for the hydrophobic blocks before PEG coupling in acetone-D_6.

Table S2. CMA incorporated into hydrophobic blocks via RAFT copolymerization based on the integrations shown in Figure S5.

Polymer	Yield (%)	Aromatic/alkene ratio	CMA/Styrene	CMA:styrene	Total CMA composition
P(S-*stat*-CMA)$_{56}$	21	17.61	0.34	1:2.92	0.26
P(S-*stat*-CMA)$_{70}$	19	17.68	0.34	1:2.94	0.25
P(S-*stat*-MA)$_{104}$-	25	18.21	0.33	1:3.04	0.25
P(S-*stat*-CMA)$_{118}$	20	17.07	0.36	1:2.81	0.26
P(S-*stat*-CMA)$_{136}$	24	16.71	0.37	1:2.74	0.27
P(S-*stat*-CMA)$_{170}$	27	13.50	0.49	1:2.03	0.32
P(S-*stat*-CMA)$_{206}$	24	15.95	0.39	1:2.59	0.28

Synthesis and characterization of PEG-*b*-P(S-*stat*-CMA)-*b*-PEG

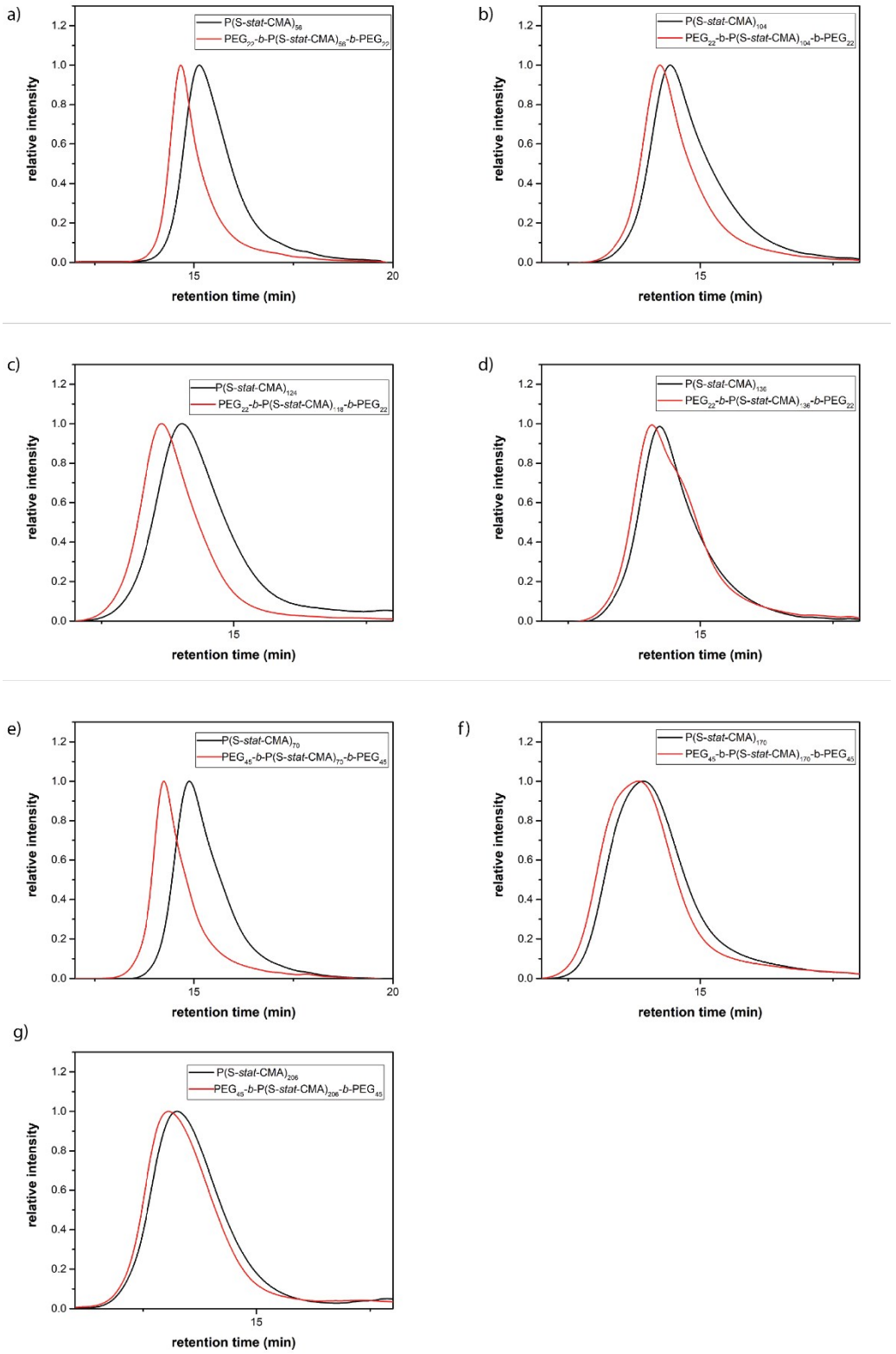

Figure S6. SEC plots (dRI detector) of the 7 triblock copolymers and their corresponding hydrophobic blocks.

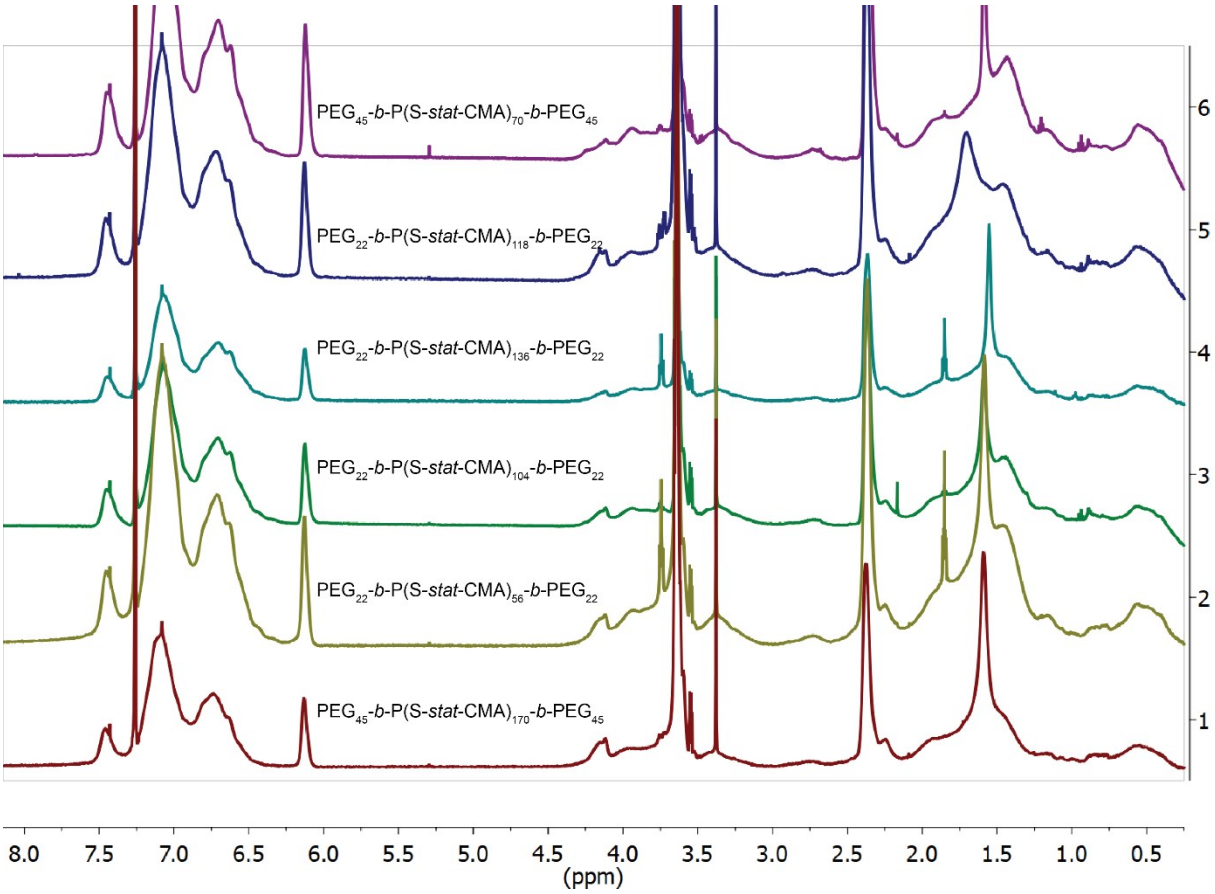

Figure S7. ^{1}H NMR spectra of the corresponding triblock copolymers whose SEC traces are shown on Figure S6 above.

Analysis of coupling via ^{1}HNMR analysis

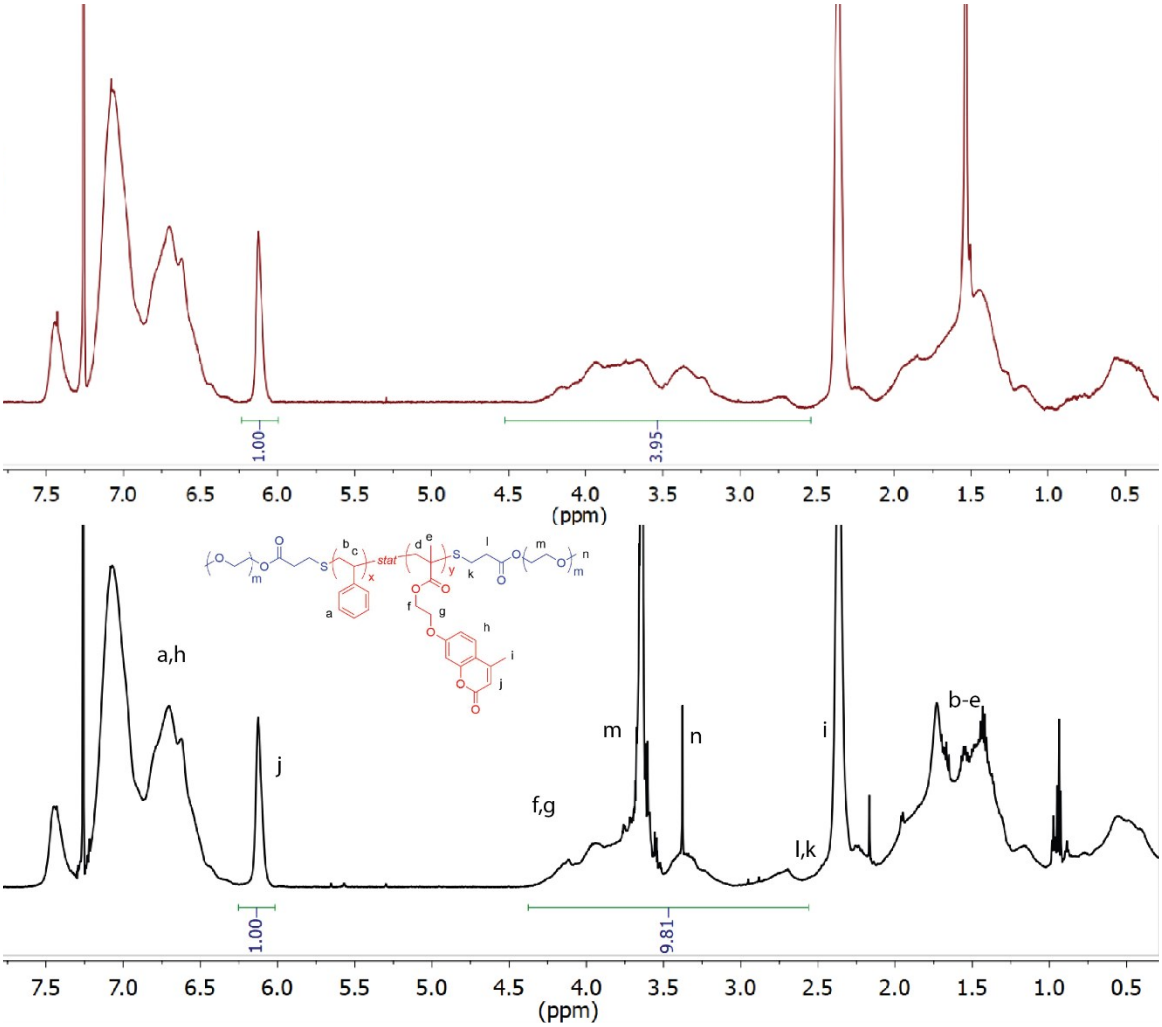

Figure S8. ^{1}H NMR spectra of the (top) hydrophobic block P(S-*stat*-CMA)$_{206}$ and (bottom) its corresponding triblock copolymer, PEG$_{45}$-*b*-P(S-*stat*-CMA)$_{206}$-*b*-PEG$_{45}$.

We determined the hydrophilic fraction by comparing the integration of the alkene peak (j) to the PEG peaks 3.64 (m) and 3.38 (n). Since the PEG peaks are in the same region as some of the P(S-stat-CMA) peaks such as the methylene bridge peaks from CMA, we first removed the P(S-*stat*-CMA) contribution. Taking PEG$_{45}$-*b*-P(S-*stat*-CMA)$_{206}$-*b*-PEG$_{45}$ as an example, we

subtract 3.95 to 9.81 (Figure S8) to access the corresponding integration for the PEG peaks. The calculation is described below:

Taking the coumarin signal as integrating for one proton, we have

$$integration\ ratio\ = 9.81 - 3.95\ =\ 5.86$$

By SEC, we have:

$$M_{\text{n P(S-}stat\text{-CMA)}} = 32\ 000 \text{ g/mol}$$

And by definition:

$$M_{\text{n P(S-}stat\text{-CMA)}} = DP_{\text{CMA}} * MW_{\text{CMA}} + DP_{\text{S}} * MW_{\text{S}}$$

with $MW_{\text{CMA}} = 288.10$ g/mol and $MW_{\text{S}} = 104.15$ g/mol

We also know from the ^{1}H NMR of P(S-*stat*-CMA) that:

$$DP_{\text{CMA}} \sim 0.28 * (DP_{\text{S}} + DP_{\text{CMA}})$$

We therefore find:

$$DP_{\text{CMA}} = 57.36 = \#_{\text{CMA alkene protons/chain}}$$

And from ^{1}H NMR, we get that:

$$\#_{\text{PEG protons}} = 5.86 * \#_{\text{CMA alkene protons/chain}}$$

$$\#_{\text{PEG protons}} = 336.14$$

From this we can calculate DP_{PEG}:

$$DP_{\text{PEG}} = \frac{336.14\ (total\ protons) - 3\ (methyl\ protons)}{4\ (protons\ per\ repeat\ unit)}$$

$DP_{\text{PEG}} = 83.29$

Total Mass of PEG present $= 83.29 \times 44.05 \frac{g}{mol} (repeat\ unit\ MW) =$ 3665 g/mol

PEG weight fraction $f = \frac{3665}{8500 + 3665} = 0.10$

Note that, for the sake of simplicity, our calculation is approximate in that we purposefully ignore the loss of the trithiocarbonate group (which is replaced by a thioether) and we omit the addition of the hydroxyethyl acrylate moiety.

Table S3. Analysis of PEG-*b*-P(S-*stat*-CMA)-*b*-PEG via ^{1}H NMR.

Polymer	M_n (g/mol)	CMA[a] content	PEG/ alkene	M_n (g/mol)	M_n[b] (g/mol)	PEG fraction
PEG_{22}-*b*-P(S-*stat*-CMA)$_{56}$-*b*-PEG_{22}	8 500	0.25	12.69	10 500	10 500	0.19
PEG_{22}-*b*-P(S-*stat*-MA)$_{104}$-*b*-PEG_{22}	15 500	0.25	7.34	17 500	17 500	0.12
PEG_{45}-*b*-P(S-*stat*-CMA)$_{118}$-*b*-PEG_{45}	18 000	0.26	6.94	20 300	20 000	0.11
PEG_{22}-*b*-P(S-*stat*-CMA)$_{136}$-*b*-PEG_{22}	20 900	0.27	4.90	22 800	22 900	0.08
PEG_{45}-*b*-P(S-*stat*-CMA)$_{70}$-*b*-PEG_{45}	10 500	0.25	17.11	13 800	14 500	0.24
PEG_{45}-*b*-P(S-*stat*-CMA)$_{170}$-*b*-PEG_{45}	27 800	0.32	5.89	31 300	31 800	0.13
PEG_{45}-*b*-P(S-*stat*-CMA)$_{206}$-*b*-PEG_{45}	32 000	0.28	5.86	35 700	36 000	0.10

[a]Note that these numbers are rounded up but the real numbers are used in the subsequent calculations. [b]Based on the SEC molecular weight assuming 100% completion of thia-Michael coupling.

Table S4. Summary of molecular weight characterization via SEC

	Hydrophobic block			**Triblock copolymer**		
Polymer	M_n	M_w	d*n*/d*c*	M_n	M_w	d*n*/d*c*
PEG_{22}-*b*-P(S-*stat*-CMA)$_{56}$-*b*-PEG_{22}	8500	9 400	0.154	12 500	13800	0.1289
PEG_{22}-*b*-P(S-*stat*-MA)$_{104}$-*b*-PEG_{22}	15 500	17400	0.168	19 500	21 600	0.098
PEG_{22}-*b*-P(S-*stat*-CMA)$_{136}$-*b*-PEG_{22}	20 900	23617	0.166	23 400	23 400	0.143
PEG_{45}-*b*-P(S-*stat*-CMA)$_{70}$-*b*-PEG_{45}	10 500	11700	0.155	12 200	13 800	0.125
PEG_{45}-*b*-P(S-*stat*-CMA)$_{118}$-*b*-PEG_{45}	18 000	19800	0.1482	21 600	23 500	0.114
PEG_{45}-*b*-P(S-*stat*-CMA)$_{170}$-*b*-PEG_{45}	27 800	32 500	0.1515	27 700	32 700	0.158
PEG_{45}-*b*-P(S-*stat*-CMA)$_{206}$-*b*-PEG_{45}	32 000	39400	0.1833	31 500	37 800	0.175

While the SEC traces (Figure S6) show a shift in the retention time, the SEC-MALLS results above do not reflect the corresponding changes in molecular weight. We attribute this to the wide variability observed in the d*n*/d*c* values of these polymers determined online at three angles, and we expect that a more rigorous offline determination of the d*n*/d*c* will improve this polymer molecular weight characterization.[1]

Characterization of the assemblies with DLS, TEM & UV-vis spectroscopy

The decay rate depends linearly on the square of the scattering vector, q^2 as shown on Figure S9 below. The gradient of the plot in this linear relationship is the diffusion coefficient, D, based on Fick's law (Equation S2). This diffusion coefficient is related to the particle size via the Stokes-Einstein equation (Equation S3) also shown below.[2]

$$\Gamma = Dq \qquad [S2]$$

$$R_h = \frac{k_B T}{6\pi\eta D} \qquad [S3]$$

Where, k_B is the Boltzmann constant, R_h is the hydrodynamic radius, and η is the solvent viscosity.

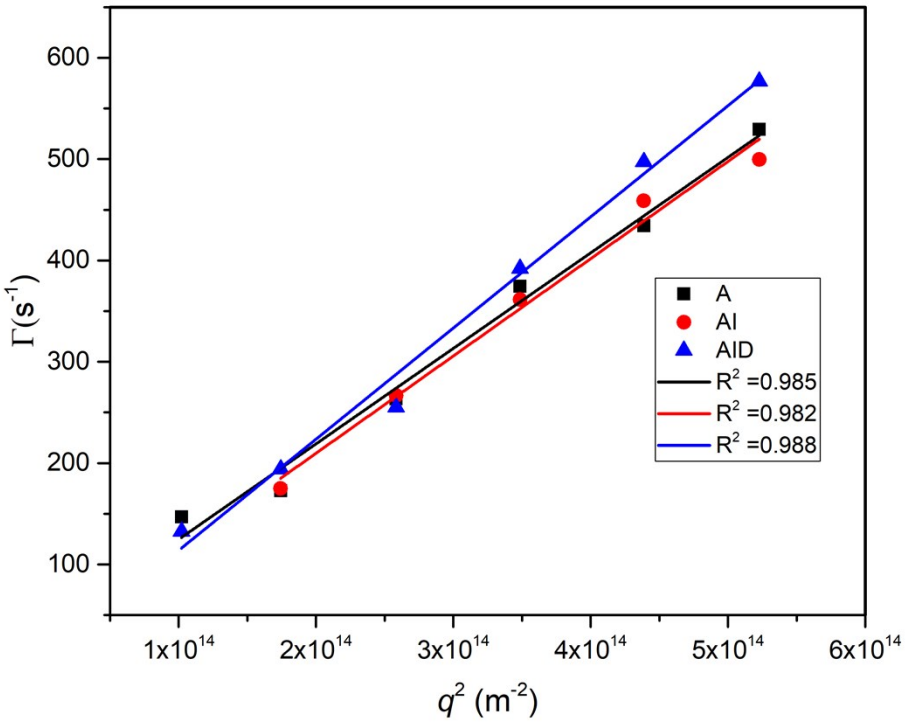

Figure S9. Derivation of the Fickian diffusion coefficient from the decay rate (Γ) and the scattering vector, q^2. The graph shows plots from DLS data collected from polymersomes after assembly (A), followed by UV crosslinking (I) and dialysis (AID).

Table S5. Comparison of DLS polymersome size at each angle vs the effective diameter from calculated multiple angle DLS.

Polymer	Rep	Expt	**45° (nm)**	**60° (nm)**	**75° (nm)**	**90° (nm)**	**105° (nm)**	**120° (nm)**	**Effective D_h (nm)**
	1	A	388	575	499	504	532	556	**517**
		AI	411	491	515	497	521	530	**494**
		AID	469	566	533	536	589	586	**546**
PEG_{45}-*b*-P(S-*stat*-CMA)$_{206}$-*b*-PEG_{45}									
	2	A[a]	417	503	479	468	502	512	**467**
		AI	390	454	475	471	474	486	**449**
		AID	454	534	506	521	561	584	**544**
	3	A[b]	360	451	463	445	458	488	**450**
		AI	391	437	458	450	478	474	**443**
		AID	393	483	477	457	563	535	**490**
	1	A[b]	360	451	463	445	458	488	**450**
		AD	328	432	436	432	441	432	**408**
		ADI	338	400	440	425	434	430	**406**
	2	A[a]	417	503	479	468	502	512	**467**
		AD	350	415	435	443	432	440	**409**
		ADI	344	412	454	446	439	437	**410**
	3	A	369	462	473	477	461	492	**450**
		AD	364	412	454	458	435	443	**411**
		ADI	390	428	491	495	471	463	**450**
PEG_{45}-*b*-PS_{403}-*b*-PEG_{45}	1	A	341	496	482	457	496	485	**462**
		AI	368	490	476	474	470	515	**454**
		AID	378	441	497	437	433	445	**397**
PEG_{45}-*b*-P(S-*stat*-CMA)$_{170}$-*b*-PEG_{45}	1	A[c]	391	488	458	453	461	500	**448**
		AI	380	442	457	458	460	482	**446**
		AID	408	490	493	482	497	540	**493**
	1	A[c]	391	488	458	453	461	500	**448**
		AD	342	416	430	413	428	440	**406**
		ADI	391	402	437	418	429	439	**402**

[a,b,c]Indicates the same vesicle suspension.

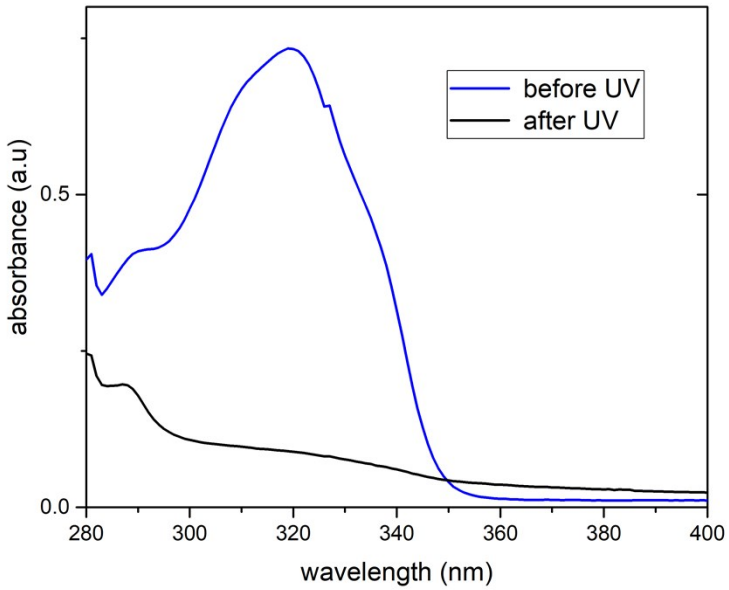

Figure S10. UV-Vis spectra of the vesicle solution before and after irradiation with UV light to induce coumarin dimerization. The vesicle solution was diluted 60-fold with THF to get a suitable concentration for analysis. The blip at 326 nm was due to the lamp change from the visible (halogen) to the UV (deuterium) light source.

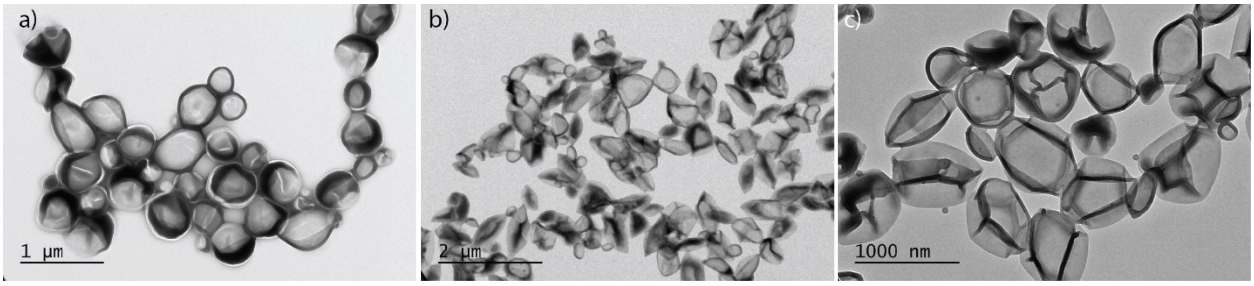

Figure S11. Dry TEM of polymersomes from PEG_{45}-*b*-P(S-*stat*-$CMA)_{206}$-*b*-PEG_{45} after (a) self-assembly (b) UV irradiation and c) dialysis after UV irradiation.

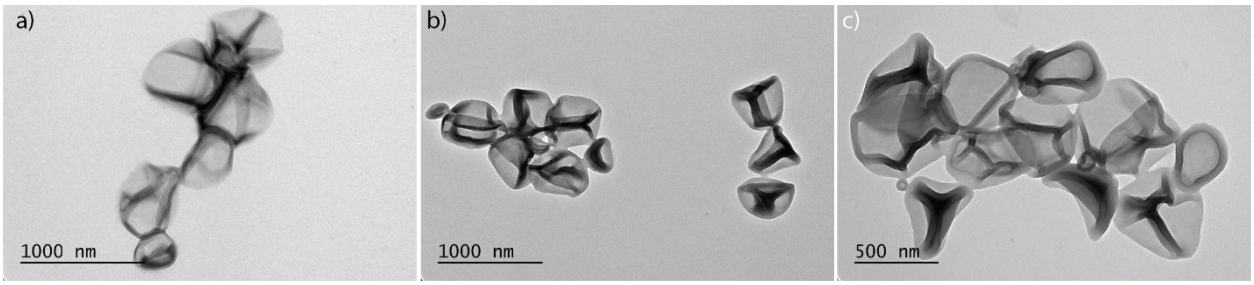

Figure S12. Dry TEM of polymersomes from PEG_{45}-*b*-P(S-*stat*-CMA)$_{206}$-*b*-PEG_{45} after (a) self-assembly (b) dialysis and c) UV irradiation after dialysis.

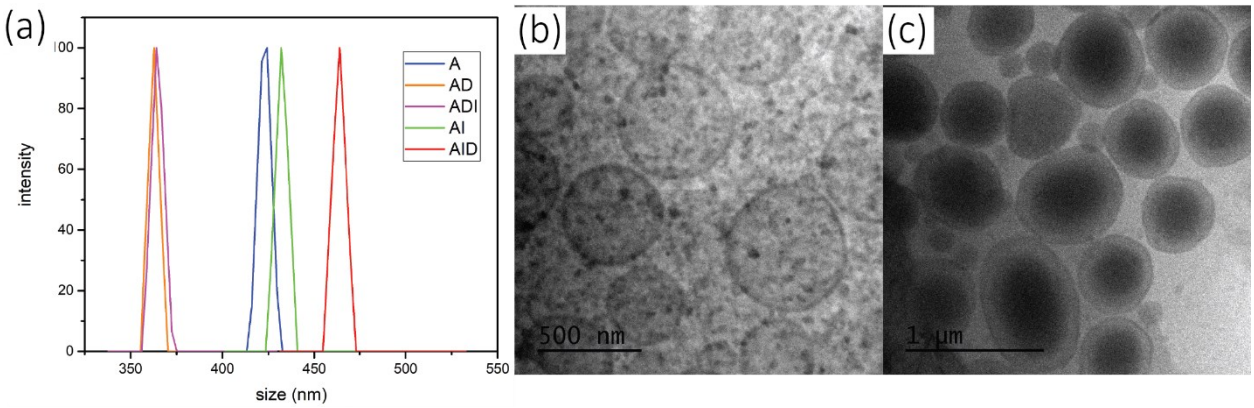

Figure S13. (a) Size distribution (at 120°) of polymersomes from PEG_{45}-*b*-P(S-*stat*-CMA)$_{170}$-*b*-PEG_{45} after each of the dialysis and irradiation procedures (b) Cryo-TEM image of the polymersome solution after dialysis (AD) and (c) after irradiation followed by dialysis (AID).

Characterization of the control PEG_{45}-*b*-PS_{403}-*b*-PEG_{45} triblock copolymer

We determined the value of *f* by comparing the integration area of the aromatic region (c on Figure S14 below) to that of the PEG methylene (d) and methyl (e) peaks as demonstrated below.

M_n= 42 000 g/mol based on SEC

Degree of polymerization $= \frac{42\,000}{104.15(S\ MW)} = 403.26$

Protons per integration unit $= 403.26\ (DP) \times 5(aromatic\ proton) = 2016.3$

Total PEG protons $= 0.16\ (aromatic{:}PEG) \times 2016.3 = 322.61$

Number of PEG units $= \frac{322.61\ (total\ PEG) - 3(methyl\ peak)}{4(protons\ per\ repeat\ unit)} = 79.90$

Total PEG weight $= 79.90 \times 44.05\ (MW\ of\ PEG\ repeat\ unit) = 3519.7$ g/mol

Therefore, PEG fraction $\frac{3519.7}{(3519.7 + 42\,0000)} = 0.08$

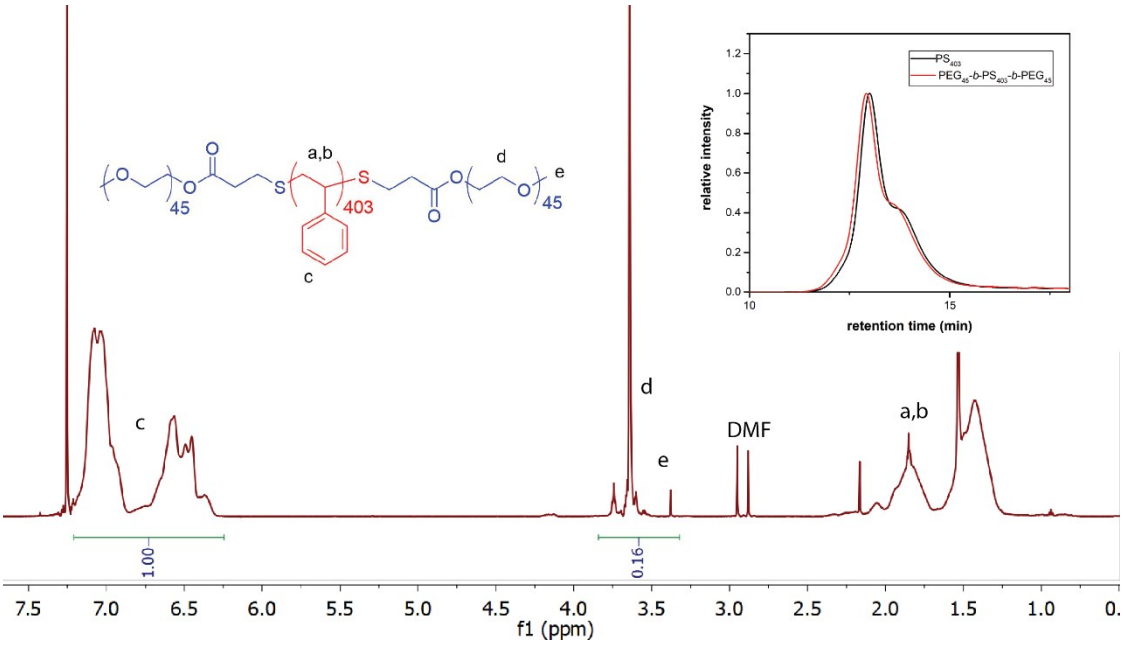

Figure S14. ^{1}H NMR spectra of the control triblock copolymer, PEG_{45}-*b*-PS_{403}-*b*-PEG_{45}.

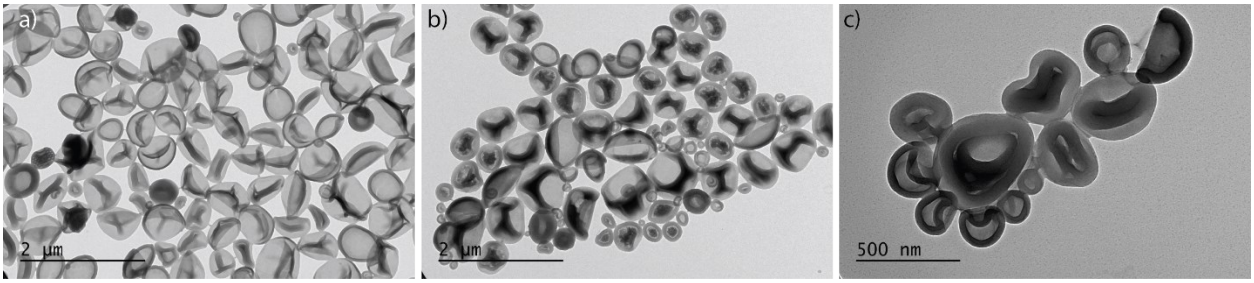

Figure S15. Dry TEM of polymersomes from PEG_{45}-*b*-PS_{403}-*b*-PEG_{45} after (a) self-assembly (b) UV irradiation and c) dialysis after UV irradiation

Dialysis of crosslinked polymersomes under hypertonic conditions

To carry out this investigation, we first divided a vesicle solution from the self-assembly of PEG_{45}-*b*-P(S-*stat*-CMA)$_{170}$-*b*-PEG_{45} into two parts. We dialyzed the first portion against a solution of NaCl (50 mM) to probe the polymersome response to hypertonic environments. We then irradiated the second portion first before dialyzing it against the salt solution under the same conditions to investigate whether the crosslinking would also affect the vesicle hypertonic behavior. The uncrosslinked polymer vesicles showed a decrease in the hydrodynamic size as expected (Figure S16a). On the other hand, the irradiated vesicle solution showed two distributions, both with sizes higher than their initial vesicle size upon assembly. When we imaged the solutions via dry TEM (Figure S16b-d), we still observed the vesicles in both solutions. This suggested that the higher distribution was likely due to vesicle aggregation. These two distributions were consistently observed over all angles. To further probe this hypertonic response, we carried out the same hypertonic test procedure using a lower concentration salt solution (25 mM NaCl). We observed the same behavior (Figure S17a), with a decrease in size on the uncrosslinked vesicles and two distributions observed in the crosslinked vesicles. The TEM images (Figure S17b-d) also suggested that the vesicle still retained their shape at this lower salt concentration. While these results once again confirm the effect of crosslinking on our polymer vesicles, in our future work, we will use cryo-TEM imaging to probe the direct morphological changes induced by these hypertonic conditions.

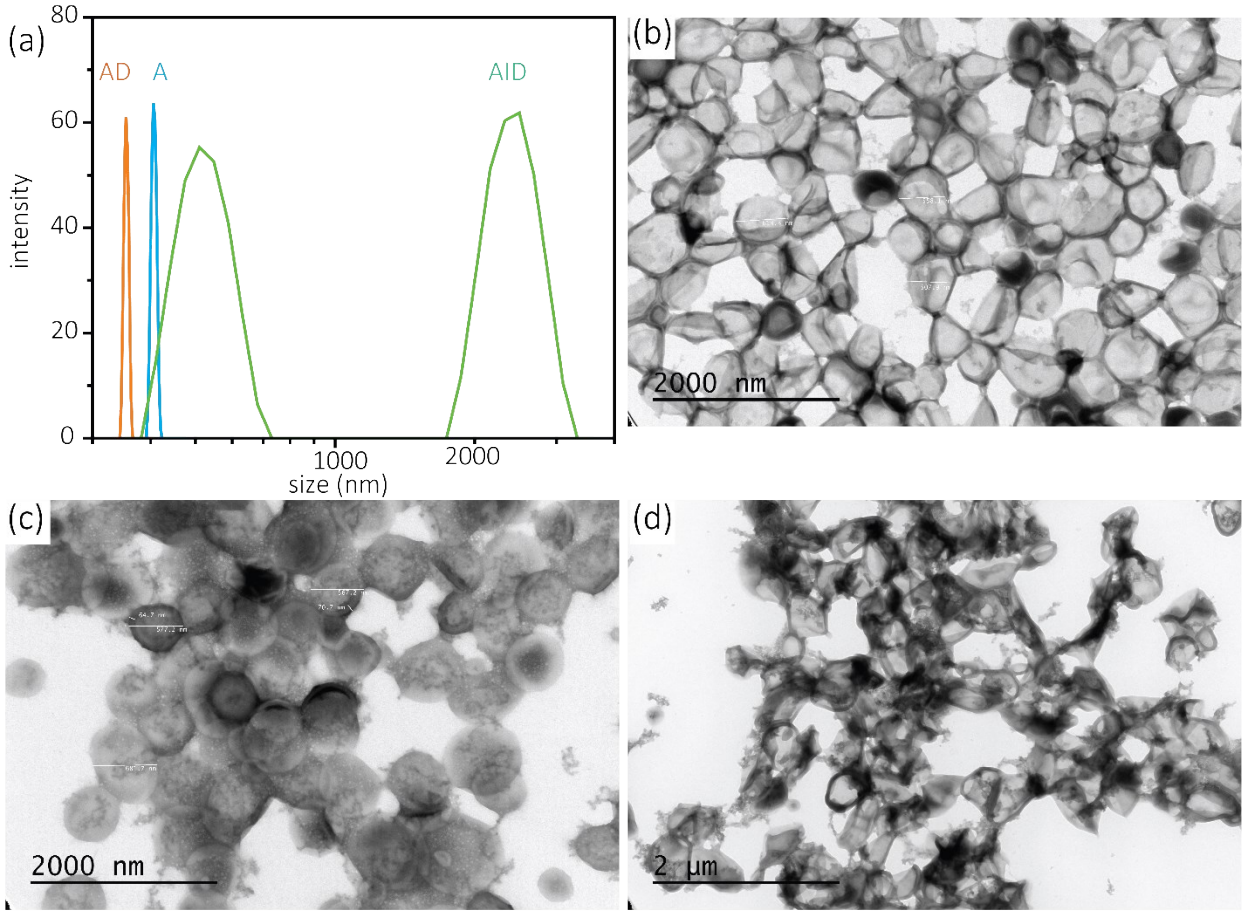

Figure S16. (a) Size distribution (at 90°) of polymersomes from PEG_{45}-*b*-P(S-*stat*-CMA)$_{170}$-*b*-PEG_{45} dialysis against salt solution (50 mM NaCl) with (AID) and without (AD) irradiation. Dry TEM images of the polymersome solution after (b) assembly, (c) dialysis against salt solution without (AD) and (d) with irradiation (AID).

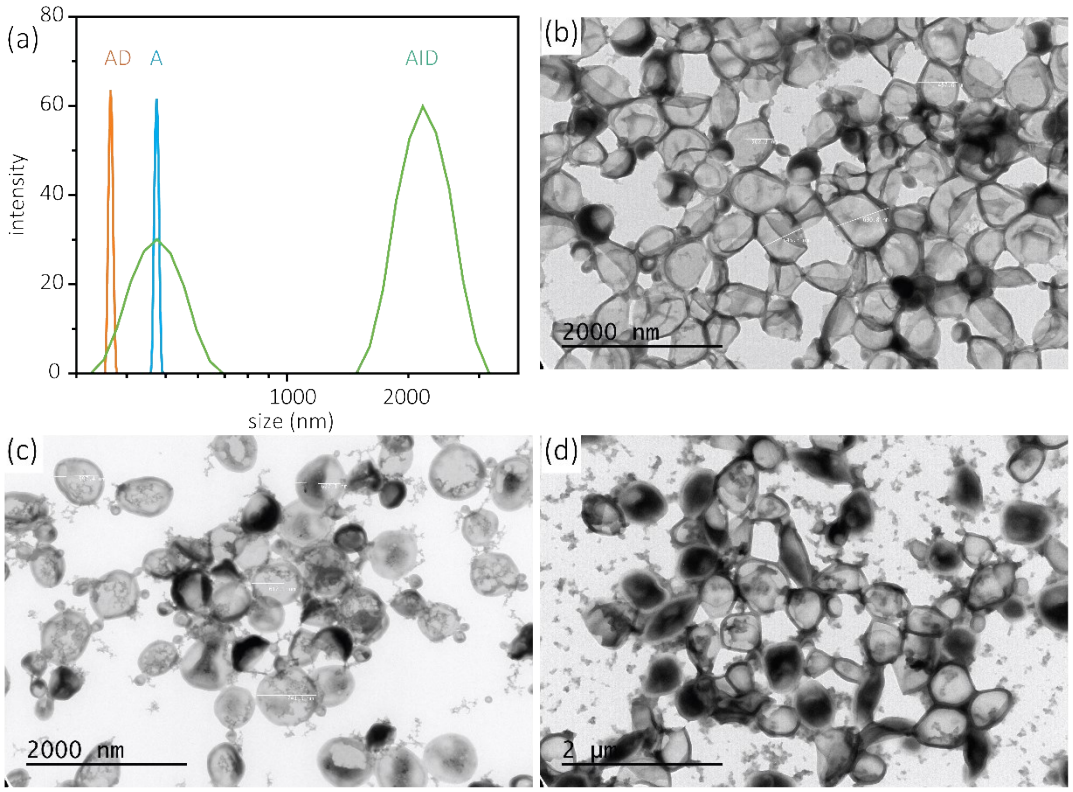

Figure S17. (a) Size distribution (at 90°) of polymersomes from PEG_{45}-*b*-P(S-*stat*-CMA)$_{170}$-*b*-PEG_{45} dialysis against salt solution (25 mM NaCl) with (AID) and without (AD) irradiation. Dry TEM images of the polymersome solution after (b) assembly, (c) dialysis against salt solution without (AD) and (d) with irradiation (AID).

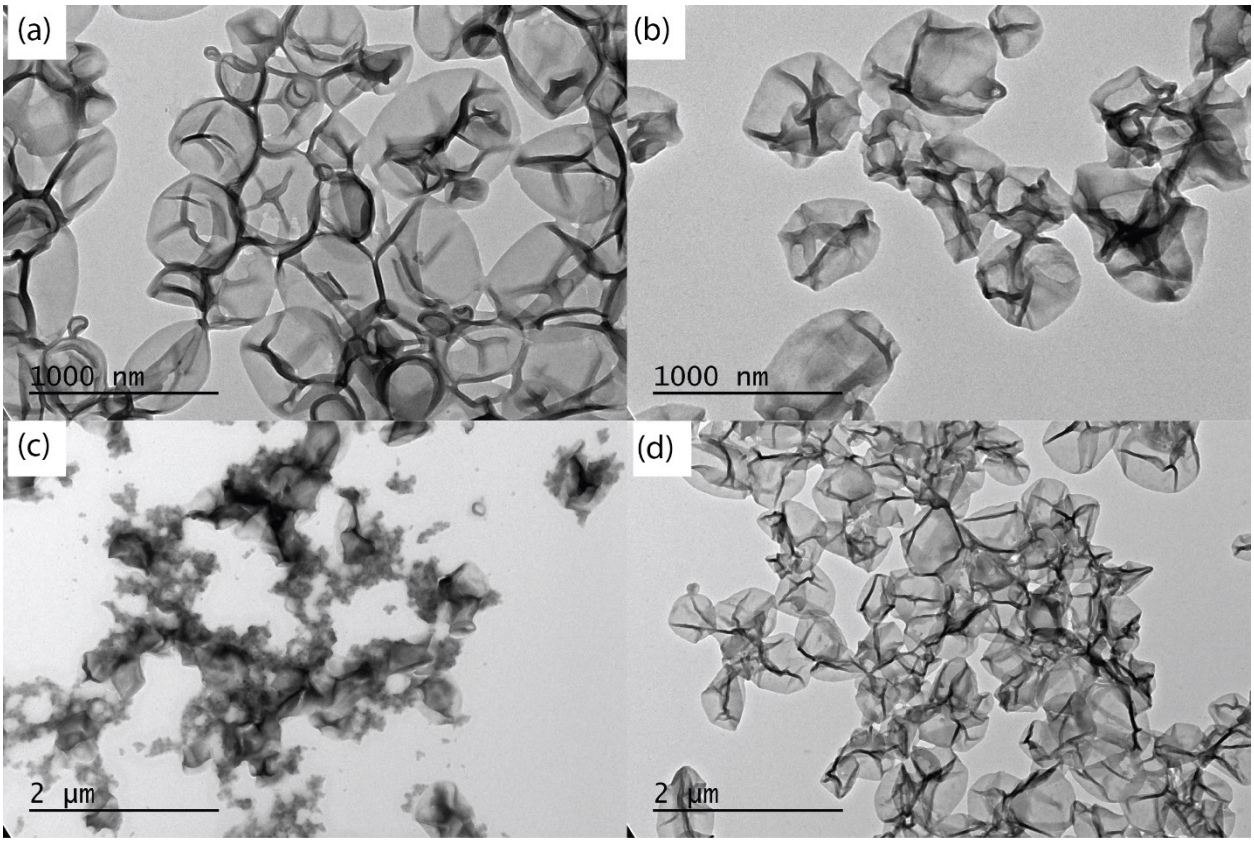

Figure S18. TEM images showing the effect of rapid osmotic pressure changes on crosslinked polymersomes. Morphologies observed after (a) assembly, (b) crosslinking (c) addition of PEG at 1 mg/mL, (d) 5 mg/mL.

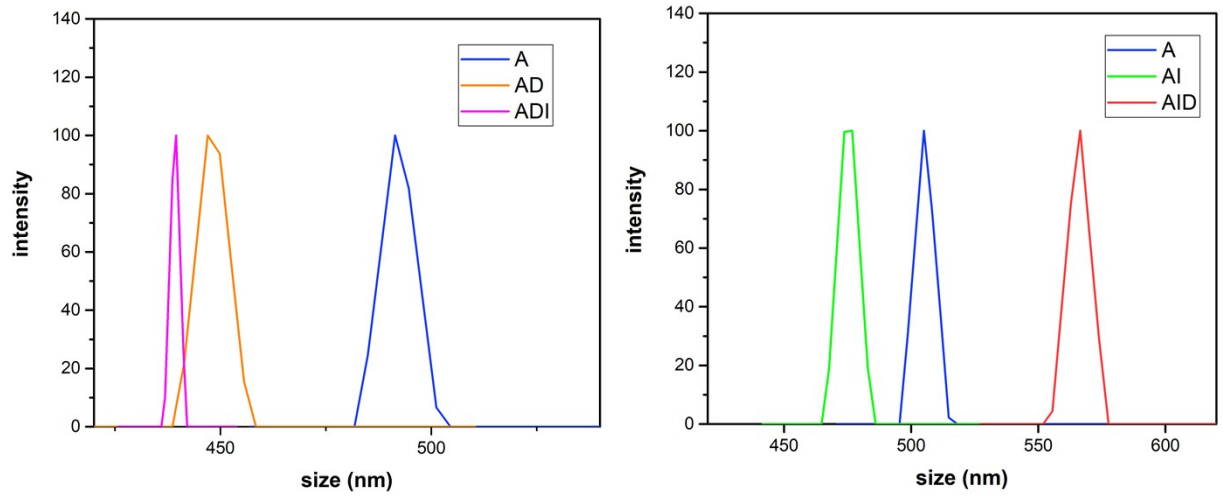

Figure S19. Original size distribution plots for showing a) the effect of dialysis (AD) followed by crosslinking (ADI). (AID). b) the effect of crosslinking (AI) followed by dialysis. The distributions smoothened using the Adjacent-Average method are shown in Figure 2a and 2c respectively.

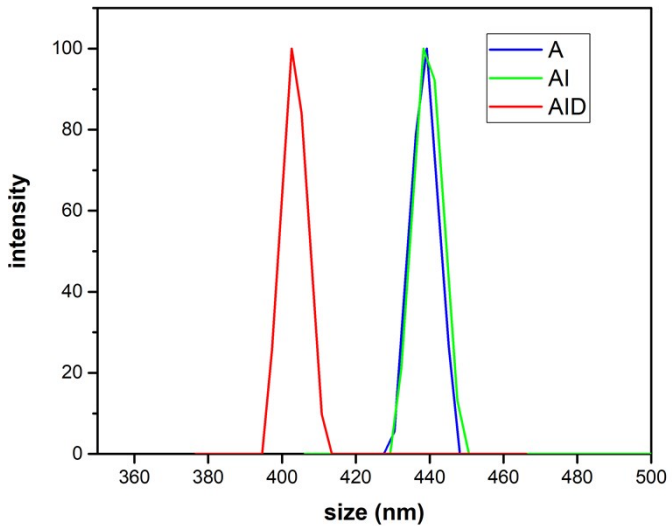

Figure S20. Original size distribution plots for showing the effect of crosslinking (AI) followed by dialysis (AID) on polymersomes from PEG_{45}-*b*-PS_{403}-*b*-PEG_{45}. The distributions smoothened using the Adjacent-Average method are shown in Figure 3b.

1. Striegel, A. M., Specific refractive index increment (∂n/∂c) of polymers at 660 nm and 690 nm. *Chromatographia* **2017,** *80* (6), 989-996.
2. Lebleu, C.; Rodrigues, L.; Guigner, J.-M.; Brûlet, A.; Garanger, E.; Lecommandoux, S., Self-Assembly of PEG-b-PTMC Copolymers: Micelles and Polymersomes Size Control. *Langmuir* **2019,** *35* (41), 13364-13374.